EFFECT OF PARASITIC PLASMA CURRENTS ON SOLAR-ARRAY POWER OUTPUT

Stanley Domitz and Joseph C. Kolecki
NASA Lewis Research Center

SUMMARY

Solar-array voltage-current curves are calculated by assuming the existence of parasitic loads that consist of local currents of charged particles collected by the array. Three cases of interest are calculated to demonstrate how the distribution and magnitude of parasitic currents affect output. Solar-array performance degradation became significant when the total parasitic current plus the load current exceeded the short-circuit current. Approximate graphical methods were useful for many applications. Power loss, which was calculated by summing the product of parasitic current and the local potential, underestimated the loss in maximum power.

INTRODUCTION

Higher powered spacecraft now being considered for future mission requirements may have solar arrays of much higher voltage output than those used in the past. The interaction of high-voltage solar arrays with a charged-particle environment has been the subject of previous study (refs. 1 to 5). The problem considered here is the effect of a parasitic load on the voltage-current output curve of the solar array itself. The parasitic load, which is actually the external collection of ambient charged particles falling on exposed conductors of the solar array, degrades useful array power output.

The collection of charged particles can arise from (1) interaction between the solar array and the ambient space plasma and (2) interaction between the array and the low-energy plasma emitted from an onboard ion source, such as an electric thruster.

The overall effect on the solar array of parasitic-current collection is to change the effective operating point of the array: For a given required load current the solar array will operate at a lower voltage and therefore at a lower power output. The current at each individual solar cell is the sum of the normal load current, which passes equally through all the cells in a series string, and the parasitic current, which varies at each cell. The parasitic current is, in general, a function of the cell potential, its position on the solar array, and the ambient plasma conditions. If the individual solar-cell current is known, its voltage can be calculated from the characteristic voltage-current curve for the type of solar cell used. The total array voltage is then the sum of the individual cell voltages. A computer program was written to

perform these summations and thus to obtain the full solar-array voltage-current curve for various conditions of interest.

Solar-array voltage-current curves were calculated for three cases of interest, representing three mechanisms for parasitic current collection:

(1) Parasitic current collected uniformly over the entire array - This one-dimensional model simplifies calculations since the parasitic current at each cell is a constant and is not affected by cell potential or array geometry. The physical situation is that the plasma sheath is small in relation to the solar-array dimensions.

(2) Parasitic current collected as a function of distance from a fixed source - The local source in this case is the charge-exchange plasma emanating from an electric thruster.

(3) Parasitic current as a function of potential - This corresponds to the infinite-sheath case, where the collected current depends on the local solar-cell potential.

The problem of parasitic currents arises normally only for high-voltage arrays such as those being considered for high-power operation. At the usual array voltages (<100 V), the parasitic current is a small fraction of the array current and is therefore not observed. For voltages in the multikilovolt range, there is a compound voltage effect - the addition of parasitic current in long series strings and the enhancement of collected current through growth of the collecting plasma sheath.

SYMBOLS

A	cell area
I	current out of string (load current)
I_L	load current, A
$I_{p,N}$	total parasitic flux falling on array, mA
i	current in solar cell, mA
i_{mp}	current at maximum power, mA
i_o	reverse saturation current, mA
i_p	parasitic flux, mA/cm^2
i_{pc}	parasitic flux, i_pA, mA/cell
i_{sc}	short-circuit current, 125 mA (assumed)

N	number of cells in series
V	voltage across string (load voltage), V
ΔV	local potential of solar cell measured from zero reference
v	voltage across solar cell, V
v_{mp}	voltage at maximum power, V
v_{oc}	open-circuit voltage (0.6 V assumed for one solar cell)

GENERAL CALCULATIONAL SCHEME

Computer Calculations

For the general case of N solar cells in a series connection (C_1, C_2, . . ., C_m, . . ., C_N), the load current I_L passes through each cell and through the load (fig. 1(a)). The parasitic currents $i_{pc,1}$, $i_{pc,2}$, $i_{pc,3}$, . . ., $i_{pc,n}$ are collected externally by each cell, as shown in figure 1. The currents are additive so that each cell carries the sum of the parasitic currents collected from the cells ahead of it in the string. The total current is

$$I_L + \sum_{\zeta=1}^{m} i_{pc,\zeta}$$

at the m^{th} cell and increases until, at some point in the string, short-circuit current is reached. At short-circuit current, the solar-cell voltage drops to zero. The remainder of the cells in the string are also at zero voltage, and they act merely as a current-carrying wire.

The potential of each solar cell is computed as a function of the current passing through it. For the calculations in this paper a simple diode type of expression is used (ref. 6):

$$v = K[\ln(i_{sc} + i_o - i) - \ln i_o] \qquad (1)$$

where v is the solar-cell potential, i is the solar-cell current (load current plus parasitic current), i_o is reverse saturation current, and K is a constant. The basic cell used in this paper is 2 centimeters by 2 centimeters with an open-circuit voltage of 0.6 volt and a short-circuit current of 0.125 ampere. In practical applications, equation (1) can be replaced by a more complicated expression involving temperature, or the solar-cell curve can be represented by a set of experimental data points. In either case the individual

solar-cell potential is obtained as a function of current and the total array potential is found by summing individual cell voltages:

$$V = \sum_{K=1}^{N} v_K$$

Therefore, to solve for the solar-array voltage-current curve, the required inputs are

(1) The array geometry - the number of solar cells in series and in parallel

(2) The distribution of parasitic current collected on the array

(3) The voltage-current curve for an individual cell

The most difficult problem is to obtain the distribution of parasitic current. In this paper only simple forms for parasitic current are used, but in general the current collected will be a complicated function of cell potential and array geometry. The method of computer calculation is described in more detail in appendix A of this paper.

Analytical Method

It is possible to obtain an analytical solution under certain conditions. For a solar-cell voltage-current curve of the form given in equation (1) and for an equal distribution of parasitic current over the array, the total array potential can be given as follows (ref. 2)

$$V = \frac{K}{i_{pc}} (A \ln A - B \ln B - Ni_{pc}) - KN \ln i_o$$

where

$$A = i_{sc} + i_o - i$$

$$B = i_{sc} + i_o - i - Ni_{pc}$$

Graphical Method

In addition to computer calculations, a graphical method can be used for most cases of interest. The graphical solution is based on a simple approximation. It is assumed that each solar cell is either "on" at some average constant voltage or "off" at zero voltage in a saturated state. This requires a rectangular solar-cell voltage-current curve. Determining the total array voltage becomes a matter of determining how many cells are generating power

and choosing an average potential for each cell. The graphical method is discussed further in appendix B of this paper.

Floating Array

The calculations for positively and negatively biased arrays are identical except that, in general, the current collection density will be smaller for the negatively biased arrays that are collecting ions. The floating condition for a solar array requires that the zero potential point of the array adjust itself so that no net current is collected; that is, the collection of ions equals the collection of electrons. To meet the floating requirement, an iterative procedure can be used to equalize the total flux of positive and negative currents. In balancing currents, the spacecraft conducting-area must be taken into account. For the floating array, those cells driven to short-circuit saturation are grouped together on the solar array at the location of floating potential, rather than at the endpoint of the array (fig. 1(b)).

RESULTS

Case 1 - Parasitic Currents Distributed Uniformly over Solar Array

The voltage-current curves of the array calculated with the methods described in the preceding section are shown in figure 2. Parasitic flux per cell i_{pc} is a parameter. The upper set of curves in figure 2 represents a series string of 40 000 cells; the lower set of curves represents a string of 4000 cells. Increasing the number of solar cells in series with constant parasitic flux decreases the fraction of useful array power because of the additive effect of the collected current. An interesting feature of figure 2 is that the right sides of the curves are almost straight lines emanating from $I = i_{sc}$. The reason for this is that in this region, cells are going into short-circuit condition at a linear rate as load current is increased, dropping the overall potential monotonically.

In figure 2 the parametric curves are given as parasitic current per cell. Relating this number to local plasma conditions would require consideration of a large number of variables such as the possibility of front and back current collection, local plasma density, ram and wake effects, magnetic field effects, and the influence of many factors on the location of the array floating point. Such factors have not been considered here; instead, the emphasis is on finding the reaction of the solar array to a given parasitic current distribution.

In figure 2 the solar-array current given represents that for a single string of cells. For a number of strings in parallel the current is proportional to the number of parallel strings. For example, with 100 parallel cells the labeled currents in figure 3 are multiplied by 100, but the array potentials remain the same.

The ratio of maximum power with parasitic current to maximum power without parasitic current is shown in figure 3 as a function of the number of cells in series with constant flux as a parameter. Essentially, the maximum-power points are replotted from data like those shown in figure 2. As expected, for a given parasitic current, the maximum-power ratio decreases with increasing string length. For a floating array, figure 3 represents the number of cells in a series string that could be either positive (collecting electrons) or negative (collecting ions). Figure 3 shows that for calculations where parasitic currents are collected in a thin sheath, the drop in maximum power is small for a floating array (where the array is primarily negatively biased) even in the ionosphere.

The voltage-current curve for a case 1 problem obtained by the graphical method is shown in figure 4. On the original solar-array curve a current $I_{p,N}$, the total parasitic flux falling on the array, is marked off on the abscissa from $I = i_{sc}$ toward the origin. A straight line is drawn from i_{sc} to the point where the original curve crosses $i_{sc} - I_{p,N}$. The graphical method is explained in more detail in appendix B of this paper.

Case 2 - Current Collection from Local Source

For the calculation of current collection from a local source, the source of charged particles is the charge-exchange plasma from an electric thruster exhaust beam (ref. 7). Charge-exchange ions drift away from the beam to create a bridge that enables electrons to be collected by the solar array. A directly coupled array is always at positive polarity. Since the volume of charged-particle production is small and distances to the array are large, the current flux to the array falls off rapidly with distance, as shown in figure 5.

The solar-array power is 25 kilowatts, divided into two equal wings of 12.5 kilowatts each, 4.2 meters wide and 26.8 meters long. The maximum potential is 1200 volts, directly coupled to the thruster. The solar cells are arranged so that the zero-voltage point is inboard and the maximum voltage is at the outboard tip of the arrays. One wing consists of 200 000 cells, 2000 cells in series and 100 cells in parallel.

For calculation purposes, the array is divided into 10 equal sections, as shown in figure 5. The parasitic current to each segment is obtained from the data of reference 7 and is considered to be constant in the section. Within each section, the calculation of the total section voltage proceeds as in case 1. The overall potential is obtained by adding voltages of the 10 sections.

Figure 6 shows the resulting voltage-current curve. The total collected parasitic current is approximately 25 percent of the solar-array current, and the decrease in maximum-power point is about 18 percent, as shown in figure 6. Because most of the parasitic current is collected at low voltage for this configuration, the effect on the array is minimized. The parasitic current distribution, however, is sensitive to the model chosen for charge-exchange

ion flow. At the present time, the details of such flow for a cluster of electric thrusters have not been fully investigated.

A graphical method can again be used. Within each solar-array segment, the parasitic flux is considered to be constant. The voltage-current curve of each segment is obtained graphically in the same manner as in case 1. The resultant graph is made up of a series of straight-line segments that can be replaced with a smooth curve that approximates the true voltage-current curve.

Case 3 - Parasitic Current as Function of Potential

For the two previous cases the collected current was considered to be one-dimensional, consisting of the ambient particle flux falling on the solar array. There was no enhancement of current collected due to the effect of the local potential. To study the effect of voltage-enhanced currents on the solar-array power output, the collected currents were assumed to be of the form

$$i_{pc} = i_p A\left(1 + \frac{V}{V_{th}}\right) \tag{2}$$

Equation (2) represents the infinite-sheath case, or "orbit limited" current collection for a spherical probe. Equation (2) is approximately correct for a plain-disk probe. It is not strictly correct for large surfaces because of the intersection of particle trajectories with the array; however, trajectory calculations agree with exact calculations within a factor of 2.

The resultant voltage-current curves are shown in figure 7. Equation (2) is used to represent parasitic current for an array of 4000 cells in series with flux density as a parameter. In figure 7 the right slopes of the curves are no longer straight lines because of the nonlinear parasitic current collection. For a given parasitic flux the loss in power is much greater than for the thin-sheath case. This is due to the multiplying factor of solar-cell potential in this case. Since parasitic current for this example is proportional to voltage, the calculated power used in collecting current is proportional to voltage squared.

The next logical example to consider would be the thick-sheath case, where the effect of space charge has been taken into account. Such a computation has not been attempted because of the lack of an easily manipulated model of current collection at individual cell locations. Approximate space-charge-limited current models have been attempted (refs. 1, 6, and 8) by using geometrical figures such as flat plates, spheres, and cylinders. But for our calculations it is necessary to determine exactly where the current is collected. Another complicating factor of the finite-sheath case is that the collection of current does not increase linearly with solar-array area, and therefore the results would not be in the form of a generalized voltage-current curve.

Approximate graphical methods apply to voltage-enhanced currents also. Again the solar array is divided into segments, each with an average voltage. If the current collection is known as a function of voltage, each section can

be drawn in the same manner as in case 2. The total curve again is obtained by connecting the line segments.

DISCUSSION OF RESULTS

If the parasitic current distribution on the solar array is known, whether or not to proceed with voltage-current curve calculation depends on the particular problem. One reason for generating the voltage-current curve is to find the operating point on the curve and to determine the power available more accurately. For example, it is often necessary to know the power at the maximum-power point. The power lost to parasitic currents is usually defined as the summation over the array of the product of the parasitic currents and the potential at which they are collected. Although this is a useful number, it can be misleading. For example, in figure 4, the calculated power loss for the thin-sheath case is equal to the cross-hatched area (areas under the curve represent power). Under parasitic load the new maximum power is at point B; the original maximum power of the array is at point A. The power lost is therefore the power at A - minus the power at B, or about twice the calculated value. The reason for this discrepancy can be seen by examining figure 4. Because of the degradation in the shape of the voltage-current curve, maximum power - which is represented by the rectangle of greatest area that can be drawn under the curve - is reduced more than anticipated. There is a further reduction in power if the array must be operated at a voltage or current other than the maximum power point. Thus the "true" power-loss determination depends on requirements for the overall system.

Another interesting example concerning power loss is the case 2 result, interaction with an onboard electric thruster. Here, because of the distribution of charge-exchange ions, parasitic currents are largest at the inboard sections of the solar array (fig. 5). If the total flux to the array is increased, the power loss does not increase linearly. The reason for this is that once the lower potential cells saturate and drop to zero voltage an increase in parasitic flux has no effect on those particular cells. Although no general rule has been found to relate the calculated power loss to the "actual power loss," the calculated power loss is usually lower. If this value is unacceptable, there is little reason for going through the full array calculations.

Another measure of solar-array degradation due to parasitic currents is the sum of the total currents involved, the load current plus the total parasitic current. If this sum is greater than the solar-array short-circuit current, some degradation must be present. The reason for this is that total current, the sum of load current and total parasitic current, must pass through the last cell in the string of cells shown in figure 1. When the total current exceeds the short-circuit current of that cell, the cell is driven to zero potential. Further increase in current drives more cells into saturation and the array voltage begins to drop rapidly. An approximate way to arrive at the total array potential is to consider the array of N cells to consist of m

solar cells "on" at some average voltage v_{av} and n cells "off" at zero voltage. The array total voltage is

$$V = mv_{av}$$

This method is used when

$$I_L + \sum_{\zeta=1}^{N} i_{pc,\zeta} \geq i_{sc}$$

The graphical method discussed earlier is based on this idea and is discussed further in appendix B of this paper.

The following simple examples illustrate the use of this idea:

(1) Positively biased array (electron flux, 10^{-6} A/cm^2, an ionospheric condition; solar-cell short circuit, 0.30 A/cm^2) - If I_L is 27 milliamperes, $i_{sc} - I_L = 3$ milliamperes. Thus, 3 milliamperes is the margin that can be used up before the last cell in a string saturates, a margin of 3000 cells in series. If there were 4000 cells in series at these conditions, 1000 cells would be saturated at zero potential and 3000 cells would be at v_{av}. The total array voltage would then be 3000 v_{av}.

(2) Floating array with 10 000 cells in series - a good approximation is to assume that the array is entirely negative. If the ion flux is 10^{-8} ampere per cell, the load current is 27 milliamperes, and the margin is 3 milliamperes, the total parasitic current is 0.1 milliampere, not enough to saturate any cells. Therefore there is little effect on array potential.

For a floating array the assumption used in the preceding example, that the voltage-current curve of the negative portion of the array can be used as the entire array curve is a convenient starting point. Accurate calculation requires the addition of two curves, one for the positively biased section and one for the negatively biased section. However, iteration is required because the floating point shifts in the process and greatly increases the amount of computation required.

An unusual effect occurs when some of the solar cells on a floating array are driven into saturation. In this case, there is a group of cells at zero potential located at the floating point. As the array orientation changes the floating point, and consequently the group of saturated cells moves about in response to the changing external conditions, the effect is similar to shadowing of a solar array by a spacecraft protrusion such as an extended boom.

CONCLUDING REMARKS

The solar-array voltage-current curve can be calculated if the parasitic current distribution on the array is known and the individual solar-cell oper-

ating curve is given. The most difficult task at present is to formulate the current distributions.

The justification for calculating the array voltage-current curve is to obtain the operating point and power output of the array more accurately. The calculated power loss $\sum i_{pc} \Delta V$ is usually less than the actual power loss and may differ by a factor of 2 or more, depending on the operating point.

If the sum of array load current plus total parasitic current is greater than the array short-circuit current, array performance will noticeably degrade and further calculation is indicated.

An approximate solar-array voltage-current curve can be drawn by dividing the array into sections and constructing the curve from straight-line segments. The total array voltage at any load current is found from $V = mV_{av}$, where m is the number of active solar cells.

For a floating array with large enough parasitic currents, a group of cells on the array will be at zero potential and will move about as a result of changing conditions. The phenomenon is similar to array shadowing.

APPENDIX A

METHOD OF COMPUTER CALCULATION

The case of N solar cells in series with parasitic currents is shown in figure 8, where all currents are taken to be electron currents. In this figure, V is the load voltage and I is the load current. Let $i_{pc,\zeta}$ be the parasitic flux falling on the ζ^{th} solar cell. The current $i_{pc,\zeta}$ may be regarded as a function of voltage and current. The equation relating these currents is

$$I = I_{tot} - \sum_{\zeta=1}^{N} i_{pc,\zeta} \tag{A1}$$

where I_{tot} is the current flowing between the array and the ground. The equation for V involves the sum of the individual solar-cell voltages v_ζ and is

$$V = \sum_{\zeta=1}^{N} v_\zeta \tag{A2}$$

where

$$v_\zeta = K_1 \ln(i_{sc} - i_\zeta + i_o) + K_2 \ln i_o \tag{A3}$$

The term i_ζ in equation (A3) is the current flowing into the ζ^{th} solar cell and is given by

$$i_\zeta = I + \sum_{\lambda=1}^{\zeta-1} i_{pc,\lambda} \tag{A4}$$

The complete voltage-current characteristic is obtained by solving these equations. The calculations are done in two groups, each group yielding a portion of the total voltage-current curve. The first group of calculations apply to the case where some number of cells in the series string are in saturation. In this case $I_{tot} = i_{sc}$ and the term N in equations (A1) and (A2) is replaced by a variable n representing the number of active cells in the string. The variable n varies in the interval $0 \leq n < N$. The second group of calculations applies to the case where all the cells in the string are active. In this case $n = N = \text{Constant}$, and I_{tot} becomes a variable and varies in the interval $0 \leq I_{tot} < i_{sc}$. This grouping of calculations arises out of the peculiar physics of this situation. The contribution of each group of calculations to the total voltage-current curve is shown in figure 8.

APPENDIX B

GRAPHICAL CONSTRUCTION OF VOLTAGE-CURRENT CURVE WITH PARASITICS

It is initially assumed that the voltage-current characteristics of a single solar cell can be approximated by a square curve, as shown in figure 9. The voltage v^* shown in the figure as the intercept of the voltage-current characteristic with the voltage axis is defined to be a suitably chosen voltage near to the voltage at maximum power. If $I = i_{sc}$, then $V = 0$. If $0 \leq I < i_{sc}$ then $V = v^*$. If N identical solar cells are connected in series, then, for $0 \leq I < i_{sc}$, $V = Nv^*$.

The concept of parasitic currents can be introduced at this point. Suppose that parasitic current is uniform per cell; that is, suppose that $i_{pc} = \text{Constant}$. If M cells are in saturation ($I = i_{sc}$ and $V = 0$) from the effect of this parasitic, $V = (N - M)v^*$. Since M is a variable, for the portion of the curve corresponding to the case of cells in saturation, V is a linear function of M. For the case of no cells in saturation, the remainder of the curve is given by $V = Nv^*$. The characteristic is drawn so that the current intercept is at short-circuit current i_{sc}.

The graphical method of constructing the voltage-current characteristic of N cells in series with $i_{pc} = \text{Constant}$ can now be developed. The voltage-current curve without parasitics is taken as the starting point. This curve is a rectangle with current intercept i_{sc} and voltage intercept Nv^*.

A threshold current i_{co} is introduced such that, if $0 \leq I < i_{co}$, then N cells are active and, if $i_{co} < I < i_{sc}$, then some number $M \leq N$ of cells is in saturation because of the presence of the parasitic i_{pc}.

For any current I in the interval $i_{co} < I \leq i_{sc}$, the number M is found as follows: The requirement is set that $I + (N - M)i_{pc} = i_{sc}$. Then $(N - M) = 1/i_{pc}(i_{sc} - I)$. But when I is in the interval $i_{co} < I \leq i_{sc}$, the voltage V is given by $V = (N - M)v^*$. Thus, in this interval

$$V = \frac{1}{i_{pc}} (i_{sc} - I)v^*$$

that is, V varies linearly with I.

Since for any current I in the interval $0 \leq I \leq i_{co}$ the voltage is $V = Nv^*$, an approximate curve can now be drawn. This curve is shown in figure 10. It is useful to find the current i_{co}. In the case of the approximation being discussed, the solution for i_{co} is quite simple. The equation $N - M = 1/i_{pc}(i_{sc} - I)$ is used at the instant $I = i_{co}$. At this instant, $M = 0$ and $i_{co} = i_{sc} - Ni_{pc}$. Thus, given a rectangular solar-array voltage-current curve, the curve with parasitic $i_{pc} = \text{Constant}$ can be constructed by drawing a straight line $V = Nv^*$. In practice, greater accuracy is obtained if the straight line drawn from i_{sc} (fig. 10) is allowed to intercept the original voltage-current curve, as shown in figure 4.

REFERENCES

1. Knauer, W., et al.: High Voltage Solar Array Study. (Hughes Research Laboratories; NASA Contract NAS3-11535.) NASA CR-72675, 1970.

2. Springgate, W. F.; and Oman, H.: High Voltage Solar Array Study. (D2-121734-I, Boeing Aerospace Co.; NASA Contract NAS3-11534.) NASA CR-72674, 1969.

3. Kennerud, K. L.: High Voltage Solar Array Experiments. (Boeing Aerospace Co.; NASA Contract NAS3-14364.) NASA CR-121280, 1974.

4. Domitz, S.; and Grier, N. T.: The Interaction of Spacecraft High Voltage Power Systems with the Space Plasma Environment. Power Electronics Specialists Conference, Institute of Electrical and Electronics Engineers Inc., 1974, pp. 62-69.

5. Herron, B. G.; Bayless, J. R.; and Worden, J. D.: High Voltage Solar Array Technology. AIAA Paper 72-443, Apr. 1972.

6. Purvis, C.; Stevens, N. J.; and Berkopec, F. D.: Interaction of Large, High Power Systems with Operational Orbit Charged Particle Environments. NASA TM-73867, 1977.

7. Solar Cell Array Design Handbook, Vol. 1. (JPL SP43-38, Jet Propulsion Laboratory; NASA Contract NAS7-100 and JPL-953913.) 1976.

8. Kaufman, H. R.; Isaacson, G. C.; and Domitz, S.: The Interaction of Solar Arrays with Electric Thrusters. AIAA Paper 76-1051, Nov. 1976.

9. Parks, D. E.; and Katz, I.: Solar Electric Propulsion Thruster Interactions with Solar Arrays. (SSS-R-78-3420, Systems Science and Software; NASA Contract NAS3-20119.) NASA CR-135257, 1977.

10. Parker, L. W.: Sheath Interaction Between an Orbiting High-Voltage Solar Array and the Space Plasma. Trans. Am. Geophys. Union, vol. 58, no. 12, Dec. 1977, Abstract p. 1215.

11. Parks, D. E.; and Katz, I.: Spacecraft-Generated Plasma Interaction with High Voltage Solar Array. AIAA Paper 78-673, Apr. 1978.

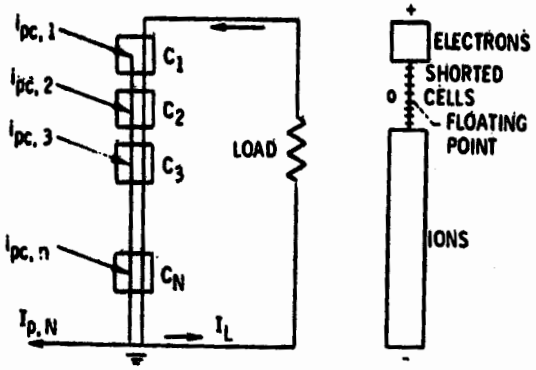

(a) Current circuits. (b) Floating array.

CS-78-1364

Figure 1. - Schematic of current systems.

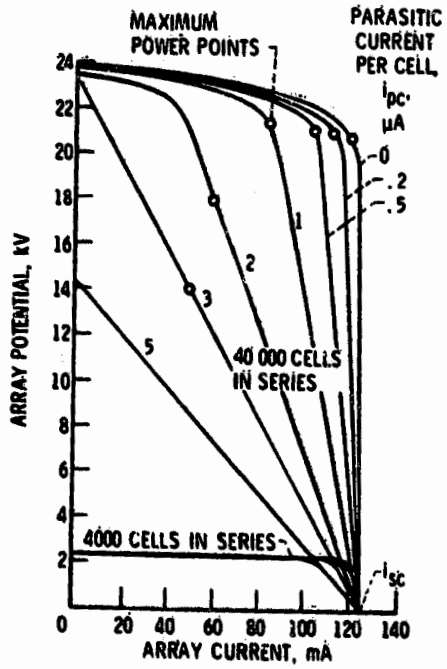

CS-78-1366

Figure 2. - Solar-array voltage-current curve with parasitic flux as parameter.

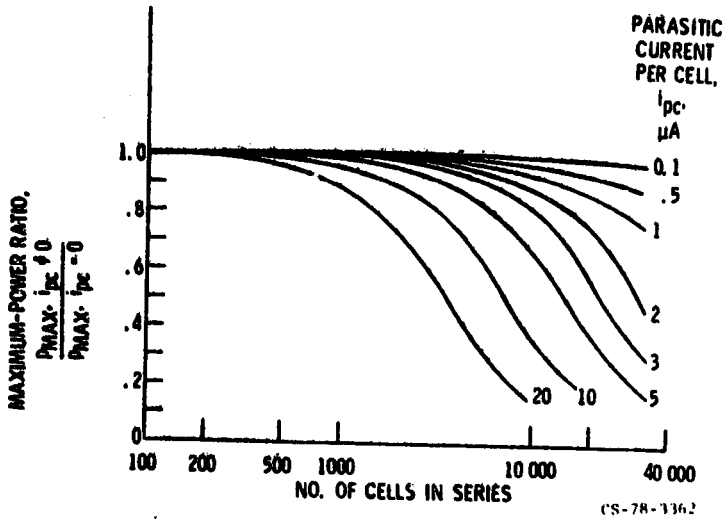

Figure 3. - Maximum-power ratio as function of number of cells in series for constant parasitic flux (thin sheath).

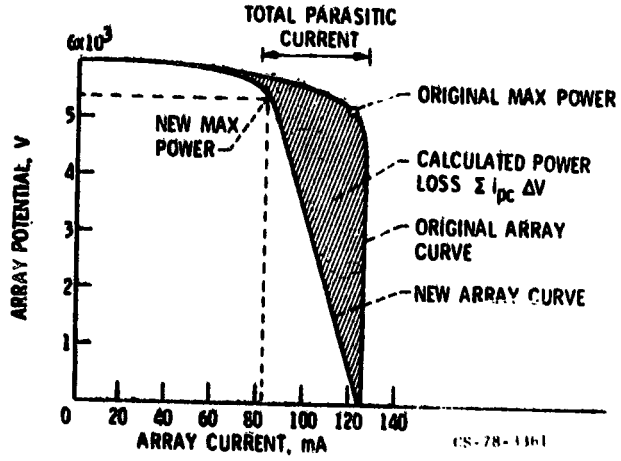

Figure 4. - Graphical construction for thin-sheath case.

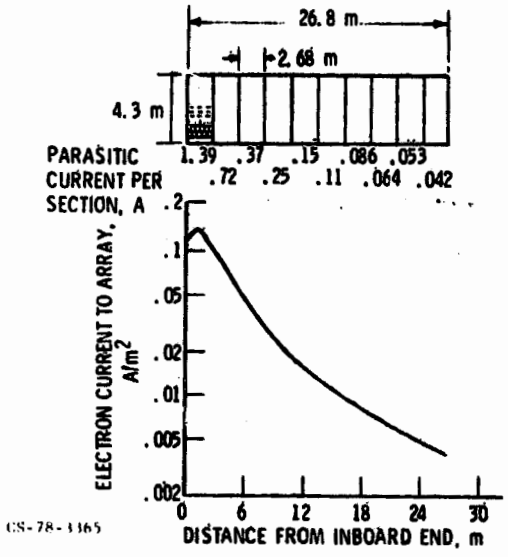

Figure 5. - Solar-array layout and parasitic flux.

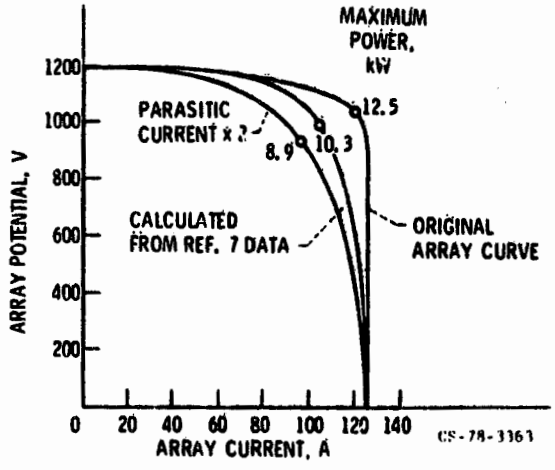

Figure 6. - Voltage-current curve for solar array - thruster integration.

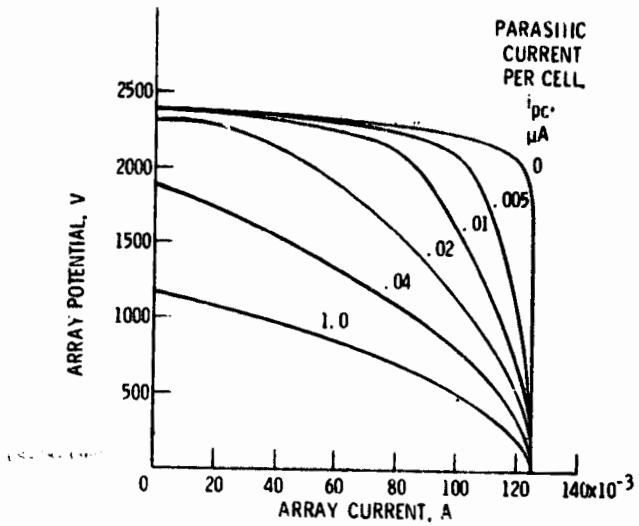

Figure 7. - Voltage-current curve for voltage-dependent current collection - 4000 cells in series.

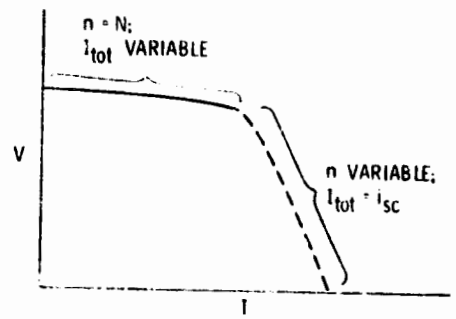

Figure 8. - Contribution of each group of calculations to total voltage-current characteristic.

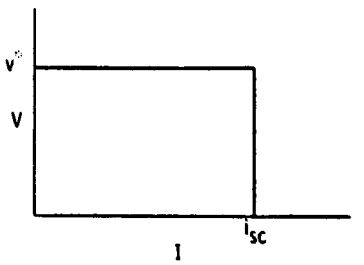

Figure 9. - Square approximation to solar-cell voltage-current characteristic.

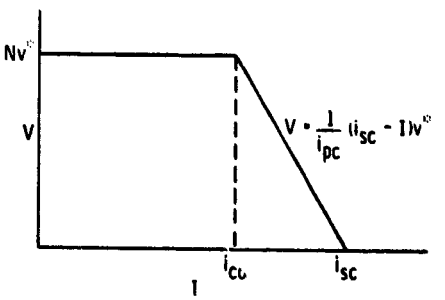

Figure 10. - Approximate voltage-current curve with parasitic flux i_{pc} constant.